ChemPubSoc Europe

DOI: 10.1002/cphc.201402709

CHEMPHYSCHEM Articles

Separation of Time-Resolved Phenomena in Surface-Enhanced Raman Scattering of the Photocatalytic Reduction of *p*-Nitrothiophenol

E. M. van Schrojenstein Lantman,[a] P. de Peinder,[b] A. J. G. Mank,[c] and B. M. Weckhuysen*[a]

Straightforward analysis of chemical processes on the nanoscale is difficult, as the measurement volume is linked to a discrete number of molecules, ruling out any ensemble averaging over rotation and diffusion processes. Raman spectroscopy is sufficiently selective for monitoring chemical changes, but is not sufficiently sensitive to be applied directly. Surface-enhanced Raman spectroscopy (SERS) can be applied for studying reaction kinetics, but adds additional variability in the signal as the enhancement factor is not the same for every location. A novel chemometric method described here separates reaction kinetics from short-term variability, based on the lack of fit in a principal-component analysis. We show that it is possible to study effects that occur on different time scales independently without data reduction using the photocatalytic reduction of *p*-nitrothiophenol as a showcase system. Using this approach a better description of the nanoscale reaction kinetics becomes available, while the short-term variations can be examined separately to examine reorientation and/or diffusion effects. It may even be possible to identify reaction intermediates through this approach. With only a limited number of reactive molecules in the studied volume, an intermediate on a SERS hot spot may temporarily dominate the spectrum. Now such events can be easily separated from the bulk conversion process by making use of this chemometric method.

1. Introduction

Surface-enhanced Raman scattering (SERS) is a novel and powerful characterization technique and slowly developing toward maturity as a tool for heterogeneous catalysis.[1] Many effects play a role in the actual SERS spectra that are observed,[2] and full understanding of the reasons for spectral fluctuations is important for practical application of reactivity studies on the scale of single catalytic particles.[3] The large enhancement effects that are associated with the phenomenon opens doors to nanoscale molecular characterization that is otherwise impossible. This resolution is present both in quantity, or the number of molecules required for characterization, and in spatial resolution, especially with techniques such as tip-enhanced Raman scattering (TERS).[2e,4] However, single hotspot measurements require consideration in their interpretation, due to the small measurement volume, but also because of their time-dependent variability.[5] Spectral fluctuations are a common feature in these time-resolved measurements.[4a, 2g,6] Due to the small number of molecules and extreme enhancement effect involved in these measurements, rare events are more readily observed where they are not (or less) visible in long time scale or bulk measurements, due to averaging over many more modes.

The interpretation of short-term variations in the spectra has been the subject of debate, as the high-enhancement field at a hotspot can also lead to photodecomposition of molecules within that hotspot.[2e,f,i] However, the spectral fluctuations are commonly explained through local changes in chemical environment around the sensed molecules, or orientation effects.[2h,6] This so-called blinking is at any rate a dynamic process, dependent on temperature and mobility of the molecules on the surface.[7] In the case of heterogeneous catalysis, short-term fluctuations might actually give valuable information about, for example, the orientations of molecules or the presence of reaction intermediates. To study these phenomena in detail, the short-lived spectral variations must be analyzed separately from long-term effects.

The near-field intensity over a SERS substrate is far from homogeneous. A few selected locations will have a very intense near-field, where other locations on the surface will hardly cause a Raman enhancement effect. This makes it an ideal technique to study any short-lived reaction intermediates that are otherwise insignificant in a bulk observation, which is best studied in few-hotspot samples to limit ensemble-averaging. Sufficiently long measurements will eventually capture the sig-

[a] E. M. van Schrojenstein Lantman, Prof. Dr. B. M. Weckhuysen
Inorganic Chemistry and Catalysis
Debye Institute for Nanomaterials Science
Utrecht University, Universiteitsweg 99
3584 CG Utrecht (The Netherlands)
E-mail: b.m.weckhuysen@uu.nl

[b] Dr. P. de Peinder
VibSpec
Haaftenlaan 28, 4006 XL Tiel (The Netherlands)

[c] Dr. A. J. G. Mank
Materials Analysis
Philips Innovation Services
High Tech Campus 11, 5656 AE Eindhoven (The Netherlands)

nature spectrum of short-lived species, as it arises at the location of an intense hotspot.

All the above effects result in spectral differences between the spectral fluctuations from the regular (bulk) spectra. Therefore, the use of chemometrics can help to separate spectra of large datasets in an effective manner. Various groups have already linked SERS measurements to multivariate analysis techniques.[8] But where signal intensity fluctuations are no problem for multivariate analysis, spectral fluctuations on various time scales can give problems in these methods.

Here, we present the use of multivariate analysis tools as an approach to separate reactivity, related to bulk changes, from short-term blinking, related to orientations, intermediate states and temporary conditions. Both are important to understand the dynamics at the catalyst particle and the developed methodology allows analysis of both effects without removal of any spectra. The chemometric method used here is a combination of principal-component analysis (PCA) and multivariate curve resolution (MCR). In PCA, the variance in a dataset is decomposed in a set of orthogonal principal components. Using only a limited number of these principal components, a large amount of variance of the input spectra can be described.[9] With MCR it is possible to decompose a mixture of spectra into their individual-component spectra.[10]

The main difference between PCA and MCR lies in the components they calculate. PCA components describe variance and can thereby also result in components with both negative and positive peaks. It is typically used as a tool to gain insight into the variance within a dataset. MCR with non-negativity constraints decomposes a set of spectra into a predefined number of spectral components, which relate to the actual spectra of the related compound. This description of a dataset with a limited number of components usually works well for the description of bulk changes. However, short-term fluctuations, like reaction intermediates, will be ignored as they are not prominent enough in the full dataset. This does not mean they are not observed. We use PCA to analyze the full dataset and separate reaction kinetics from short-term variations. These separated datasets are subsequently examined with MCR, for direct comparison to normal Raman spectra.

We present here a novel chemometric method based on PCA for time filtering (see Figure 1). Chemical reactions can hereby be separated from short-term variations, enabling better analysis of either dataset. To present this analysis method, we use a self-assembled monolayer (SAM) of *p*-nitrothiophenol (pNTP) on a flat Au substrate, as illustrated in Figure 2. SERS activity, and related reactivity, is introduced by deposition of Ag nanoparticles, similar to other experiments described in literature.[11] The monolayer of pNTP can be reduced to *p,p'*-dimercaptoazobisbenzene (DMAB) via photocatalysis over plasmonic nanoparticles, and typically uses green laser excitation and Ag nanoparticles.[3, 12] Rather than using green laser excitation, an excitation wavelength of 785 nm is chosen. This excitation excites the coupled plasmons of Au and Ag and gives sufficient enhancement effect to observe dynamics over single nanoparticle hotspots on the flat Au substrate. The choice of this low-energy excitation wavelength also ensures that the catalytic reaction is sufficiently slow to observe reactivity during the acquisition of 15 000 consecutive 1 s SERS spectra.

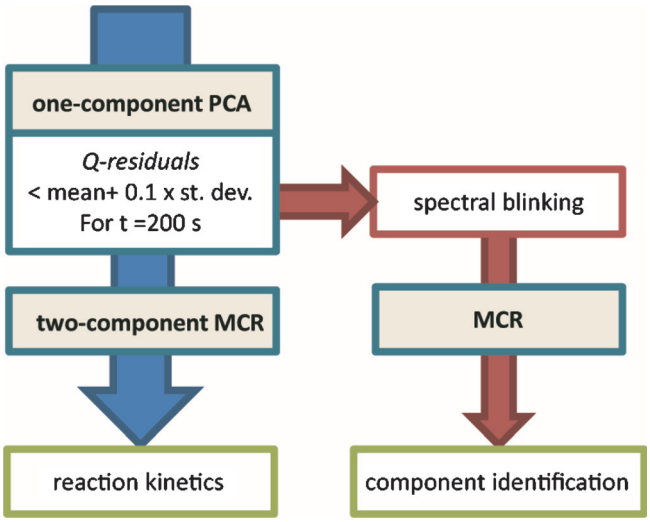

Figure 1. Workflow for the chemometric analysis of the time-resolved SERS spectra measured. A one-component principal-component analysis (PCA) is used to create a filter, separating short-term spectral blinking from reaction kinetics. Both sets of spectra can subsequently be analyzed via multivariate curve resolution (MCR).

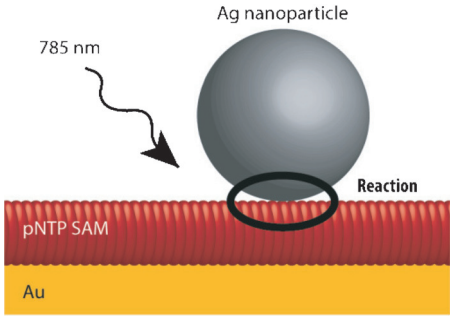

Figure 2. The experimental setup consists of single Ag nanoparticles deposited on a self-assembled monolayer (SAM) of *p*-nitrothiophenol (pNTP) assembled on a flat gold substrate. The Raman spectra have been measured at 785 nm excitation.

2. Results and Discussion

2.1. Single-Hotspot SERS

Obtaining SERS over single hotspots is achieved by deposition of single Ag nanoparticles over a pNTP-functionalized flat Au surface, as illustrated in Figure 2. A set of 15 000 Raman spectra were recorded at an excitation wavelength of 785 nm, with a 1 s integration time. Pre-processing was done via a cosmic-ray remover (WiRe 3.2, Renishaw) to remove the spikes in individual Raman spectra. These narrow peaks occur only in single Raman spectra and their removal has no effect on the time-resolved scale. The Raman spectra are analyzed for the spectral region of 1000–1635 cm^{-1}, where most vibrations characteristic

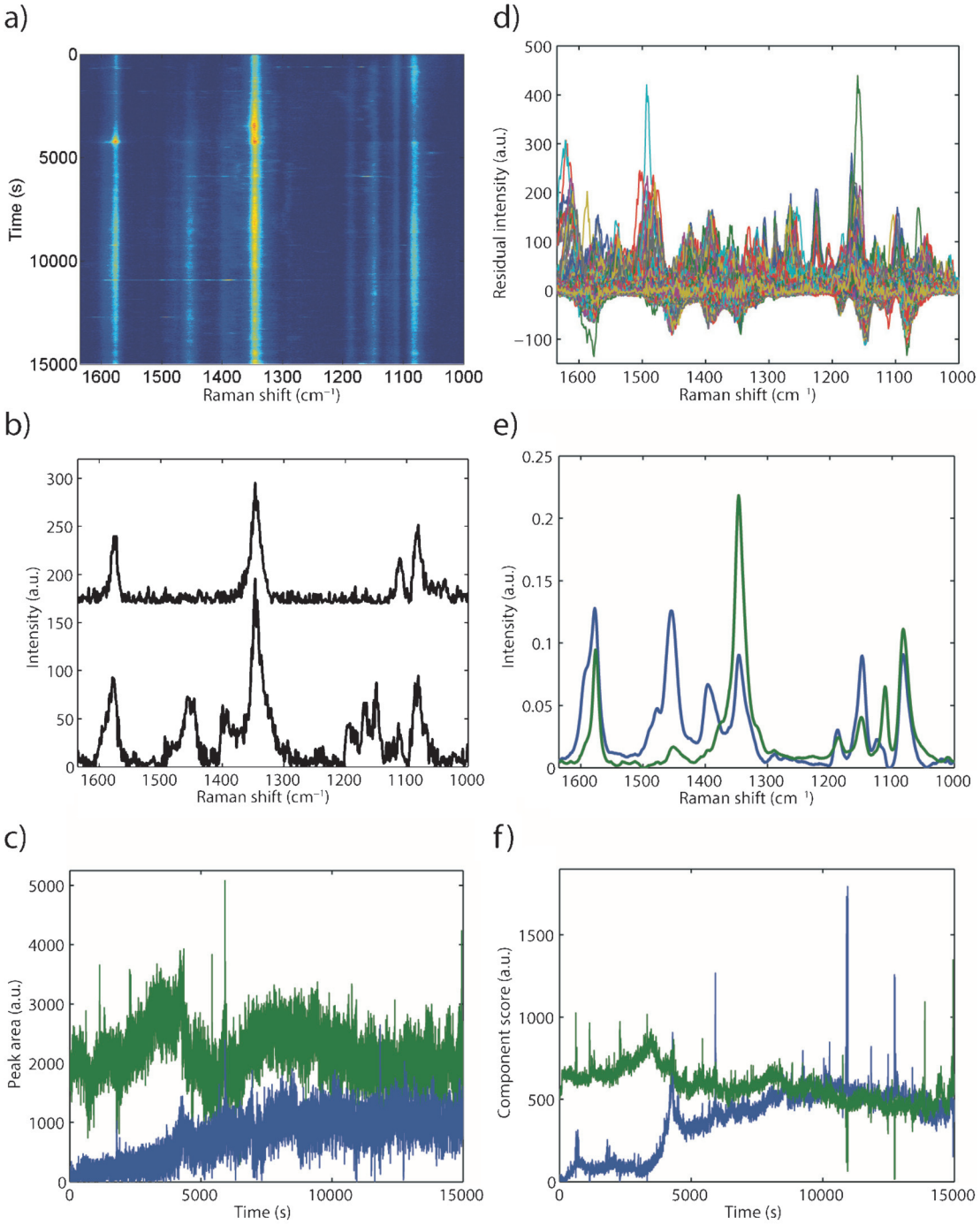

Figure 3. a) Contour plot of the Raman spectrum in time. b) First and last Raman spectrum. c) pNTP (green) and DMAB (blue) peak area as a function of time. d) Residuals after two-component MCR. e) Calculated MCR components, component 1 (green) describes 62% of the variance in the dataset, component 2 (blue) 32%, resulting in a total of 94% of the variance explained by the two-component MCR model. f) MCR scores in time.

for both reactant and product are found. A weighted least-squares (WLS) baseline correction is calculated, after which the absolute value of this dataset is taken.

The main Raman peaks of pNTP and DMAB are clearly visible in the color plot (Figure 3a), as well as in the first and last Raman spectra of the series (Figure 3b). A simple method for tracking the reaction progress is to plot peak areas of reactant and product as a function of time. Figure 3c shows the results of this approach, for the Raman peaks at 1335 (sym. NO_2 stretch)[13] and 1440 cm^{-1} (N=N stretch).[14] The main trends are visible: the DMAB signal comes up with time, whereas the pNTP signal appears to be less affected by the reaction and suffers more from SERS-intensity variations. The noise level in the signals is rather high, most likely due to the noise in the spectra themselves, though peak shifts also contribute to the noise level. This method is sufficient for monitoring the (irre-

versible) reaction in time, but shows quite some noise in the overall signal.

MCR is a more reliable method, as it takes the full spectrum into account, rather than just a single peak. For this dataset, an unrestrained two-component MCR analysis results in a model that describes 94% of the total signal variance. Component 1 (62%, see Figure 3e) resembles the reactant very well, while the second component (32%) comprises a mixture of DMAB with a smaller contribution of pNTP. The corresponding scores in time (Figure 3f) show more detail and less noise respect to the peak area analysis method (Figure 3c). MCR can therefore be concluded to be a satisfactory method to track this reaction.

Nonetheless, the spectral residuals after MCR (Figure 3d) still show many spectral features. Blinking is a prominent feature in this dataset and occurs in spectral patterns that do not overlap with those of pNTP and DMAB. As this photoreaction encompasses multiple reaction steps,[15] these spectra can contain valuable information regarding the mechanism. In fact, when time and spatial resolution of SERS is high enough, these spectral fluctuations are expected to be the way to identify possible reaction intermediates.

2.2. Separation of Signal Variations on Different Time Scales

To separate short-term (reversible) fluctuations from the long-term reaction progress, a new method of data processing is introduced. The photoreduction of pNTP to DMAB can largely be characterized by the disappearance of the pNTP spectrum, and the rise of the DMAB spectrum. After a simple spike removal, PCA is used to separate long-term trends from short-term trends using a 200 s time filter. The exact window required for the time filter depends on the dynamics of the system and experimental parameters like acquisition time. It can be altered to suit the needs of a particular dataset.

A one-component PCA on the time series (after spike removal) results in the component and score shown in Figure 4a,b. The spectral pattern of the component shows great resemblance to the spectrum of DMAB, and describes 56% of the variance in the dataset. The score plot of this component in time is similar to that expected for a reaction, with a slow increase in loading as time progresses. Hardly any short-term fluctuations are visible.

The q-residuals in time (Figure 4d) show the sum of squares of the residual spectra, not explained by the model. They are a way of plotting lack-of-fit for all spectra. These show a stable

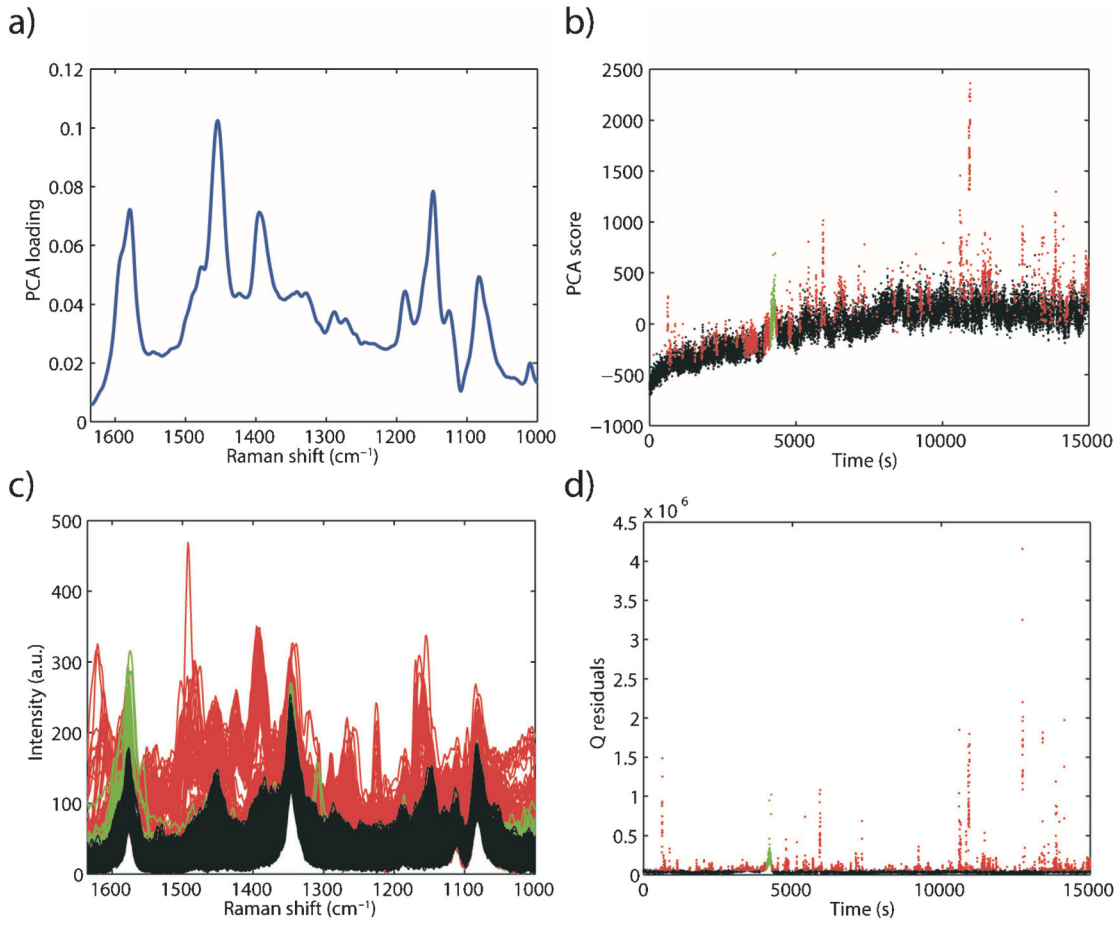

Figure 4. One-component PCA calculation of the full dataset. a) Loading of component 1 (56% variance captured), b) score of component 1 in time, c) separation of spectra into the three categories, black and green spectra describe the bulk reaction, red spectra are spectral fluctuations and will be analysed separately later. d) Q-residuals in time with 200 s filter. The datapoints are coloured as in (c).

(low) baseline, but with quite some short-term deviation from this baseline. The PCA component does not describe those spectra very well as they are present only for short periods during the total 15000 s. In other words, they show some form of spectral deviation from the bulk reaction. To separate these spectral fluctuations for closer examination, any q-residuals with a value higher than the mean value $+0.1\times$the standard deviation of all q-residuals are selected, unless they consist of a series of spectra that are above this norm for 200 s consecutively. At the start of the reaction, the PCA does not always fit the full trend of reactivity, since changes due to the reaction can result in relatively large spectral changes. However, these first spectra are only a minor part of a large dataset and thus are not accurately described by the one component PCA model. Therefore the q-residual criterion of the first 100 spectra is a five-fold higher value to ensure no reactivity information is lost.

In Figure 4d, all black data points represent spectra that have a sufficiently low q-residual value, and are taken for further analysis of bulk reaction. In this first separation, the green data points are also included. They are above the set q-residual criterion, but persistent enough to be considered as bulk processes. Red data points are below the q-residual criterion as the corresponding spectra are only present during short time intervals. They are set aside and can thus be analyzed separately from the bulk reaction. The color coding in Figure 4d is also applied to Figure 4b,c to indicate the relation between these different parameters.

Figure 4c shows the breakdown of the full set into the different sets of spectra. Black spectra fall within the Q-residual criterion and describe the reaction. Green spectra do not meet up to the Q-residual criterion, but make it through the time filter. They are likely an orientation effect due to changes in the monolayer, and are included in the analysis of the bulk reaction in Figure 5. Red spectra are set aside and are analyzed in Figure 6. The spectral pattern of these three sets is quite clear. With respect to the black spectra, the green spectra are only small deviations. In contrast, the red spectra show much more vibrational bands than observed in the black spectra.

2.3. Analysis of Bulk Surface Reaction

Having separated the photocatalytic reduction from short-term variations, each dataset can now be analyzed separately. The reaction spectra are taken through a two-component MCR, after preprocessing of the spectra by a WLS baseline correction

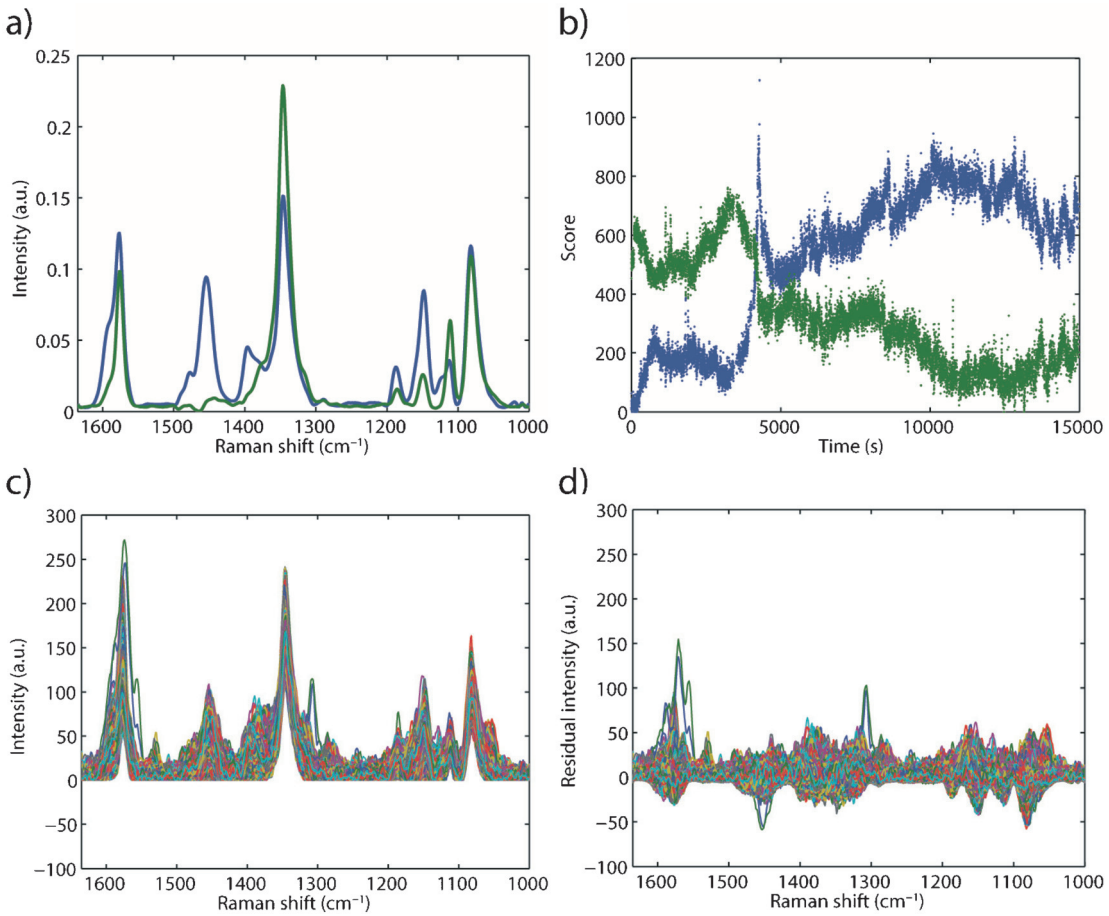

Figure 5. MCR model of all spectra belonging to the bulk reaction. In a) the two calculated components are shown. Component 1 (green) represents 27% of the calculated model, component 2 (blue) represents 70% of the calculated model, with a total of 97% variance explained. b) Shows the score of components 1 and 2 in time. c) All input spectra for the MCR model and d) the spectral residuals that are not explained by the MCR components. These two figures are shown on the same intensity scale for comparison.

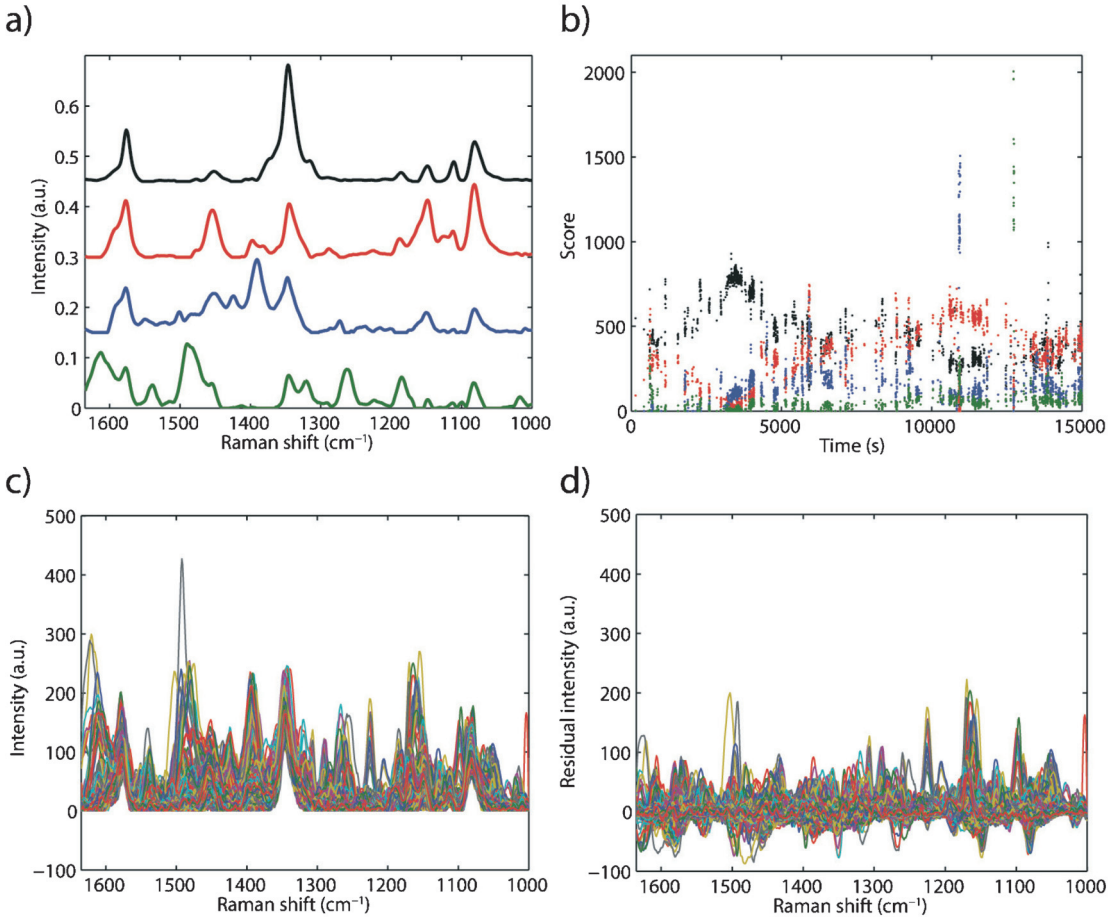

Figure 6. MCR model of all short-lived spectral components. a) The four calculated MCR components. The variance capture with the components is for black 52%, for red 24%, for blue 13%, and for green 5%. b) Score plot in time for these four components, colour-coded as for (a). c) All input spectra for this MCR analysis. d) Residuals after MCR analysis.

and taking the absolute value of the resulting spectra. Other than assuming two components to describe the reaction, no other constraints are put onto the MCR.

The calculated MCR components are shown in Figure 5a and depict pNTP (in green, 27% variance) and a mixture of pNTP and DMAB (in blue, 70% variance). The score as a function of time is shown in Figure 5b, and, like the components, rather similar to the results obtained in Figure 3e,f. The main difference is the level of noise in the score, which is lower in Figure 5b. The removal of spectral fluctuations and subsequent analysis of the pure reaction has led to better description of this reaction via MCR.

As can be expected, the variance explained by two MCR components within this filtered dataset is slightly higher (97%) than in the non-filtered dataset (94%). This is further emphasized by the input spectra (Figure 5c) and spectral residuals (Figure 5d). Less spectral fluctuations are put into the model, so less are found in the spectral residuals, when comparing Figure 5d to Figure 3d.

Overall, the time filter benefits the MCR model. But for application of this model to the description of reaction kinetics, some additional steps will have to be taken. The mixture of pNTP and DMAB in component 2 makes it difficult to determine the fraction of pNTP in the total signal. It will likely be a linear combination of both components 1 and 2. DMAB is simpler, as that is only expressed in component 2. Though the actual contribution of DMAB will only be a fraction of the score for component 2, this will be a matter of scaling the intensity and will not affect the calculation of reaction rate.

2.4. Analysis of Spectral Fluctuations

Most important in this novel chemometric method is its ability to analyze short-term spectral fluctuations in large dataset. These fluctuations are expected to give information on short-lived events on the surface of the Ag substrate, which could be either due to reorientation of pNTP or DMAB, or a reaction intermediate. Figure 4 showed how variations present for less than 200 s were separated from the long-term effects of the bulk reaction. The separated spectra that exhibit these short-term fluctuations are shown in Figure 6c. Many spectral features are present, and at varying intensities.

A four-component MCR analysis was found to describe the majority (94%) of the spectral components in this dataset. The largest component (Figure 6a,b, black, 52%)) has a maximum contribution at around 4 000 s in the dataset. It is very similar

to component 1 in Figure 5a, and is also most prominent at the beginning of the reaction. In comparison to the reactant component in Figure 5, a slight variation in peak ratios is observed, which is most likely caused by a different orientation or local environment for the reactant. Similarly, the second component (Figure 6a,b, red, 24%) has similarities to component 2 in Figure 5a, and is present at the end of the reaction. Again, the differences are in peak ratios, likely caused by molecular orientation or variations in the local environment.

The third (Figure 6a and b, blue, 13%) and fourth (Figure 6a,b, green, 5%) components have a different behavior in their score in time. Both are rather low in intensity, apart from one instance—at 11 000 for component 3, and 12 500 for component 4. The most characteristic peak in the third component is the vibration at 1380 cm^{-1}. This is a known vibration of DMAB,[14] and appears to be strongly enhanced at that specific moment.

The fourth component is hard to place in the context of either pNTP or DMAB, and could be a reaction intermediate. Reaction intermediates will have a similar molecular structure as pNTP and DMAB, but with a different functional group. The characteristic vibrations at for example, 1335 and 1440 cm^{-1} would not be expected at exactly that location in an intermediate spectrum. Also, reorientation of pNTP or DMAB molecules should not result in new vibrations with respect to the normal Raman spectrum. Though beyond the scope of this work, it is anticipated that future density functional theory (DFT) calculations should be able to shed more light on the chemical information in these spectral components.

The novelty of this chemometric method is its capability of analyzing short-lived Raman spectra. Though most deviating spectra will probably be explained via orientation effects, there is a small chance that intermediates will also be present at the intense enhancement field in a SERS hotspot, if the measurement runs long enough. Normally short-lived spectra are disregarded in the analysis of a 15 000 SERS spectra dataset, but now these spectra can be identified for the study of the surface reaction dynamics.

3. Conclusions

We have presented a new approach to the chemometrics of SERS spectra, which can find widespread use in this important field of research. It was found that with a one-step time filter with a PCA approach, the photocatalytic reduction of pNTP monitored by SERS could be analyzed in great detail. More specifically, with this PCA analysis, the photocatalytic reduction process ($>$200 s) was separated from strong spectral deviations occurring over shorter time intervals ($<$200 s). Both sets of data were then separately analyzed.

The subsequent MCR analysis on the reaction data yields less noise, compared to simple peak area analysis and to regular MCR without PCA filter. Additionally, the blinking SERS spectra separated from the bulk reaction process can now be analyzed separately. Here, a four-component MCR analysis has shown the main components of these deviating spectra.

Where the bulk reaction data cleans up nicely with the use of this filter, the real advantage is in the blinking spectra. Here, we have shown that the developed approach is able to isolate these events. If SERS is indeed going to reveal reaction intermediates, it will be most probably during sparse events. It is important to note that SERS has this inherent capability due to the inhomogeneous enhancement effect over the SERS-active substrate.

Experimental Section

Ag nanoparticles were synthesized according to Lee and Meisel[16] In short, 0.04908 g silver nitrate (Sigma Aldrich, ACS reagent, ~99.0%) was dissolved in 10 mL mQ water. 3.667 mL of this stock solution was added to 100 mL mW water in a round-bottomed flask equipped with a Teflon stirrer bar and reflux column. After heating the solution to reflux temperature, 2 mL of 0.09 M sodium citrate tribasic dihydrate (Sigma, reagent grade, ~99%) was added. After 5 min at reflux temperature, the sol had turned a yellow/brownish colour with silver reflectance. This sol was left to cool and stored in a refrigerator until required for experiments.

A flat Au substrate of 100 nm Au over a 0.5×1.0 cm Si wafer (Philips Innovation Services) was cleaned with UV/ozone and anhydrous ethanol. Subsequently, the substrate was immersed into a 10 mM ethanolic solution of pNTP (Fluka, technical grade) for 24 h, followed by threefold rinsing in 10 mL ethanol. A tenfold dilution of Ag nanoparticle sol was directly dropcasted onto the substrate and left to dry in ambient conditions.

Raman measurements were performed on a Renishaw InVia microscope, using 785 nm diode laser excitation, through a 50× long-working-distance objective. The described experiment was done using 0.25 mW laser excitation power, for 15 000 consecutive spectra at a 1 s integration interval.

Chemometric analysis was performed using the PLS Toolbox 6.71 (Eigenvector Co.) in combination with Matlab 2012a (Mathworks). Unless mentioned otherwise, raw SERS spectra were loaded directly into Matlab and smoothed with a second-order (9 pixel) Savitsky–Golay filter. A quick spike removal was done through a home-written routine: a one-component PCA (mean centre pre-processing) was analysed on the basis of the q-residuals in time. Any spectrum with a q-residual value higher than the mean $+0.1\times$ standard deviation of all q-residuals was removed if the datapoint was three times larger than its direct neighbours. A five times higher filter was used for the first 100 spectra, to cope with the start of the reaction. The result of this filtering is the separation of the total dataset in categories that relate to spectral variations on different time scales that van be linked to different physical and chemical changes on the surface.

Acknowledgements

This work is supported by the Netherlands Research School Combination—Catalysis (NRSC-C), a European Research Council (ERC) Advanced Grant (no. 321140), and NanoNextNL, a micro and nanotechnology consortium of the Government of the Netherlands and 130 partners.

Keywords: chemometrics · heterogeneous catalysis · Raman spectroscopy · self-assembly · surface-enhanced Raman scattering

[1] a) H. Kim, K. M. Kosuda, R. P. Van Duyne, P. C. Stair, *Chem. Soc. Rev.* **2010**, *39*, 4820 – 4844; b) B. Ren, G.-K. Liu, X.-B. Lian, Z.-L. Yang, Z.-Q. Tian, *Anal. Bioanal. Chem.* **2007**, *388*, 29 – 45.

[2] a) M. D. Sonntag, D. Chulhai, T. Seideman, L. Jensen, R. P. Van Duyne, *J. Am. Chem. Soc.* **2013**, *135*, 17187 – 17192; b) M. D. Sonntag, J. M. Klingsporn, L. K. Gairbay, J. M. Roberts, J. A. Dieringer, T. Seideman, K. A. Scheidt, L. Jensen, G. C. Schatz, R. P. Van Duyne, *J. Phys. Chem. C* **2012**, *116*, 478 – 483; c) R. L. Agapov, A. V. Malkovskiy, A. P. Sokolov, M. D. Foster, *J. Phys. Chem. C* **2011**, *115*, 8900 – 8905; d) E. C. Le Ru, P. G. Etchegoin, in *Principles of Surface-Enhanced Raman Spectroscopy*, Elsevier, Amsterdam, **2009**; e) K. Domke, B. Pettinger, *Phys. Rev. B* **2007**, *75*, 236401; f) C. C. Neacsu, J. Dreyer, N. Behr, M. B. Raschke, *Phys. Rev. B* **2007**, *75*, 236402; g) W. Zhang, B. S. Yeo, T. Schmid, R. Zenobi, *J. Phys. Chem. C* **2007**, *111*, 1733 – 1738; h) T. Ichimura, H. Watanabe, Y. Morita, P. Verma, S. Kawata, Y. Inouye, *J. Phys. Chem. C* **2007**, *111*, 9460 – 9464; i) C. C. Neacsu, J. Dreyer, N. Behr, M. B. Raschke, *Phys. Rev. B* **2006**, *73*, 193406; j) A. Kudelski, B. Pettinger, *Chem. Phys. Lett.* **2004**, *383*, 76 – 79.

[3] E. M. van Schrojenstein Lantman, T. Deckert-Gaudig, A. J. G. Mank, V. Deckert, B. M. Weckhuysen, *Nat. Nanotechnol.* **2012**, *7*, 583 – 586.

[4] a) T. Schmid, L. Opilik, C. Blum, R. Zenobi, *Angew. Chem. Int. Ed.* **2013**, *52*, 5940 – 5954; *Angew. Chem.* **2013**, *125*, 6054 – 6070; b) S. Kawata, *Appl. Spectrosc.* **2013**, *67*, 117 – 125; c) M. Richter, V. Deckert in *Surface and Thin Film Analysis* (Eds.: G. Friedbacher, H. Bubert), Wiley-VCH, Weinheim, **2011**, pp. 481 – 497; d) K. F. Domke, B. Pettinger, *ChemPhysChem* **2010**, *11*, 1365 – 1373; e) E. Bailo, V. Deckert, *Chem. Soc. Rev.* **2008**, *37*, 921 – 930.

[5] J. Stadler, T. Schmid, R. Zenobi, *Nanoscale* **2012**, *4*, 1856 – 1870.

[6] D. R. Ward, N. K. Grady, C. S. Levin, N. J. Halas, Y. Wu, P. Nordlander, D. Natelson, *Nano Lett.* **2007**, *7*, 1396 – 1400.

[7] a) Z. Wang, L. J. Rothberg, *J. Phys. Chem. B* **2005**, *109*, 3387 – 3391; b) Y. Maruyama, M. Ishikawa, M. Futamata, *J. Phys. Chem. B* **2004**, *108*, 673 – 678.

[8] a) B. R. Wood, E. Bailo, M. A. Khiavi, L. Tililey, S. Deed, T. Deckert-Gaudig, D. McNaughton, V. Deckert, *Nano Lett.* **2011**, *11*, 1868 – 1873; b) M. Richter, M. Hedegaard, T. Deckert-Gaudig, P. Lampen, V. Deckert, *Small* **2011**, *7*, 209 – 214; c) W. Xie, C. Hermann, K. Kömpe, M. Haase, S. Schlücker, *J. Am. Chem. Soc.* **2011**, *133*, 19302 – 19305; d) W. Cheung, I. T. Shadi, Y. Xu, R. Goodacre, *J. Phys. Chem. C* **2010**, *114*, 7285 – 7290.

[9] R. Bro, A. K. Smilde, *Anal. Methods* **2014**, *6*, 2812 – 2831.

[10] A. de Juan, J. Jaumot, R. Tauler, *Anal. Methods* **2014**, *6*, 4964 – 4976.

[11] W.-H. Park, Z. H. Kim, *Nano Lett.* **2010**, *10*, 4040 – 4048.

[12] a) E. M. van Schrojenstein Lantman, O. L. J. Gijzeman, A. J. G. Mank, B. M. Weckhuysen, *ChemCatChem* **2014**, *6*, 3342 – 3346; b) K. Kim, J.-Y. Choi, K. S. Shin, *J. Phys. Chem. C* **2014**, *118*, 11397 – 11403; c) K. S. Shin, Y. K. Cho, K. Kim, *Vib. Spectrosc.* **2014**, *70*, 120 – 124; d) T. You, L. Jiang, P. Yin, Y. Shang, D. Zhang, L. Guo, S. Yang, *J. Raman Spectrosc.* **2014**, *45*, 7 – 14; e) L. Kang, P. Xu, B. Zhang, H. Tsai, X. Han, H.-L. Wang, *Chem. Commun.* **2013**, *49*, 3389 – 3391; f) X. Ren, E. Tan, X. Lang, T. You, L. Jiang, H. Zhang, P. Yin, L. Guo, *Phys. Chem. Chem. Phys.* **2013**, *15*, 14196 – 14201; g) Z. Zhang, L. Chen, M. Sun, P. Ruan, H. Zheng, H. Xu, *Nanoscale* **2013**, *5*, 3249 – 3252; h) V. Canpean, S. Astilean, *Spectrochim. Acta Part A* **2012**, *96*, 862 – 867; i) K. Kim, K. L. Kim, K. S. Shin, *J. Raman Spectrosc.* **2012**, *43*, 228 – 236; j) M. Sun, Z. Zhang, H. Zheng, H. Xu, *Sci. Rep.* **2012**, *2*, 647; k) B. Dong, Y. Fang, X. Chen, H. Xu, M. Sun, *Langmuir* **2011**, *27*, 10677 – 10682; l) K. Kim, K. L. Kim, K. S. Shin, *J. Phys. Chem. C* **2011**, *115*, 23374 – 23380; m) K. Kim, Y. M. Lee, H. B. Lee, Y. Park, T. Y. Bae, Y. M. Jung, C. H. Choi, K. S. Shin, *J. Raman Spectrosc.* **2010**, *41*, 187 – 192; n) K. S. Shin, C. S. Park, W. Kang, K. Kim, *Chem. Lett.* **2008**, *37*, 180 – 181; o) Y. Wang, X. Zou, W. Ren, W. Wang, E. Wang, *J. Phys. Chem. C* **2007**, *111*, 3259 – 3265; p) K. Kim, I. Lee, S. J. Lee, *Chem. Phys. Lett.* **2003**, *377*, 201 – 204.

[13] B. O. Skadtchenko, R. Aroca, *Spectrochim. Acta Part A* **2001**, *57*, 1009 – 1016.

[14] Y.-F. Huang, H.-P. Zhu, G.-K. Liu, D.-Y. Wu, B. Ren, Z.-Q. Tian, *J. Am. Chem. Soc.* **2010**, *132*, 9244 – 9246.

[15] S. Sun, R. L. Birke, J. R. Lombardi, *J. Phys. Chem.* **1988**, *92*, 5965 – 5972.

[16] P. C. Lee, D. Meisel, *J. Phys. Chem.* **1982**, *86*, 3391 – 3395.

Received: October 11, 2014
Published online on December 11, 2014

